18TH WORLD CONFERENCE ON EARTHQUAKE ENGINEERING
WCEE2024
MILAN

MILAN, ITALY
30TH JUNE - 5TH JULY 2024
www.wcee2024.it

NEW FRAMEWORK FOR SEISMIC EVALUATION OF RC WALL STRUCTURES BASED ON SIMULATION AND MATERIAL STRAINS

J. Murcia-Delso[1], I. Koutromanos[2], X. Deng[3], P. Luna[4], M. Panagiotou[5], N. Duarte[4].

[1] Department of Civil and Environmental Engineering, Universitat Politècnica de Catalunya - BarcelonaTech (UPC), Barcelona, Spain, juan.murcia-delso@upc.edu

[2] Department of Civil and Environmental Engineering, Virginia Polytechnic Institute and State University, Blacksburg, United States

[3] Department of Structural Engineering, University of California, San Diego, La Jolla, United States

[4] Department of Civil and Environmental Engineering, Universitat Politècnica de Catalunya - BarcelonaTech (UPC), Barcelona, Spain

[5] Nabih Youssef Structural Engineers, Los Angeles, United States

Abstract: *Reinforced concrete (RC) wall buildings comprise a significant portion of the building inventory in regions of high seismic hazard. Seismic assessment standards in the United States (ASCE/SEI 41) and Europe (Eurocode 8-3) allow the use of nonlinear methods to evaluate this type of buildings by means of analytical models and performance thresholds defined at the component level, such as drift ratio, chord rotation or hinge rotation. The modeling parameters and acceptance limits for RC walls have been calibrated from data obtained in experiments, and they may not be accurate for wall configurations that differ from those typically used in laboratory testing. While ASCE/SEI 41 allows the use of alternative modeling parameters and limits directly obtained from physical testing of a particular component configuration, carrying out these tests can be costly and time consuming. This paper presents a novel approach for the seismic evaluation of RC wall components and building systems that combines performance criteria defined at the local (material) level and advanced computational simulation. Performance metrics based on material strains are directly related to damage mechanisms in concrete (cracking, crushing) and steel reinforcement (yielding, buckling, rupture) governing the loss of component stiffness and strength. They have the advantage of being independent of wall configuration and loading conditions. Damage criteria and strain limits for different performance levels (immediate occupancy, life safety, and collapse prevention) are proposed considering potential flexural, shear, and lap-splice failures. The successful implementation of a strain-based evaluation relies on the ability of the computational models to accurately represent material damage. Two different modeling approaches for planar walls are studied: the nonlinear truss model and a 2D continuum finite element model. Their accuracy in predicting the behavior observed in wall tests is compared and discussed, together with performance predictions obtained with ASCE/SEI 41 and Eurocode 8-3. The truss model is found to be preferable for analysis of structural systems, as it combines high accuracy with a much lower computational cost than that of continuum models. Finally, a vision for the implementation of the proposed evaluation method in engineering practice is provided.*

1. Introduction

Reinforced concrete (RC) structural walls are commonly used as lateral load resisting system of buildings in regions of high seismic hazard. RC walls can present a variety of behavior modes when subjected to severe cyclic loading, including flexure-dominated responses (with moderate to high ductility), shear-dominated responses (low ductility), as well as mixed-mode flexure-shear responses (moderate ductility). While modern design and detailing practices are intended to avoid undesired failure modes of limited ductility, structures constructed prior to the 1980s can exhibit non-ductile responses with a variety of failure modes. Flexural failures may be caused by crushing of wall toes, buckling and/or rupture of vertical steel. Shear failures may be caused by diagonal tension, diagonal compression, or shear sliding. Other possible failure modes include lap-splice sliding and local (out-of-plane) instability.

The seismic assessment standards for existing buildings in the United States, ASCE/SEI 41 (ASCE 2017), and Europe, Eurocode 8-3 (CEN 2005), allow the use of nonlinear methods to evaluate structural performance. These standards establish acceptance limits for the response of structural components (e.g. columns, walls) using component deformation measures like drift ratio or hinge rotation. ASCE/SEI 41 (ASCE 2017) classifies RC walls as flexure- or shear-dominated components, and proposes different backbone curves to represent their force-displacement responses as well as acceptance limits for performance levels that guarantee immediate occupancy (IO), life safety (LS) and collapse prevention (CP). Several backbone curve parameters and acceptance limits have been empirically established using data obtained in laboratory experiments, and they may not be accurate for actual wall configurations not resembling those used in physical testing. While the ASCE/SEI 41 (ASCE 2017) standard allows for the use of alternative model parameters and acceptance limits obtained from experimental testing of a particular component configuration, carrying out these tests can be costly and time consuming.

This paper presents a novel approach for the seismic evaluation of RC wall components and building systems that combines advanced computational simulation with performance criteria defined at the local (material) level. Performance levels based on acceptable damage in concrete and steel are defined based on the most common damage mechanisms observed in RC walls, and strain-related thresholds are proposed for these damage states. With respect to component deformation measures, material strains have the advantage of being directly related to the damage conditions affecting structural performance. Nevertheless, their use as performance indicators requires using computational simulation techniques that are capable of accurately representing these damage mechanisms. Two different structural modeling techniques are presented and discussed in this paper for the strain-based seismic evaluation of planar RC walls: the nonlinear truss model and a 2D continuum finite element (FE) model.

2. Performance criteria based on material strains

Acceptance criteria based on material strains are defined for the immediate occupancy (IO), life safety (LS), and collapse prevention (CP) performance levels of ASCE/SEI 41 (ASCE 2017). The strain limits represent damages of different intensity caused by concrete cracking and crushing, bar rupture and lap-splice slip. The proposed limits are associated to loss of stiffness and/or strength capacity of the component level. Material strain limits for IO and LS were previously proposed in displacement-based design methodologies for RC columns and walls (Priestley et al. 2007, Panagiotou and Restrepo 2011). Similar limits are adopted here for damage modes related to flexure: concrete cover spalling and large flexural cracks should be prevented for IO, while LS will be exceeded due to bar rupture or crushing of confined concrete. Additional acceptance criteria have been recently proposed by the authors in Deng et al. (2021, 2022) to consider damage modes related to shear and lap-splice failures, as well as for the CP performance level.

The three performance levels considered are defined as follows in ASCE/SEI 41 (ASCE 2017): IO corresponds to a condition for which no permanent damage has occurred and the structure practically retains its initial stiffness and strength, LS is a state for which damage is present but the structure has still a margin of safety against collapse, and for CP the structure can carry gravity loads but has not margin against collapse. Table 1 presents the list of possible damage conditions in a wall that would result in the exceedance of each performance level. Exceedance of IO corresponds to material damage that creates a noticeable loss of stiffness in the wall component: large cracking or concrete cover spalling. Exceedance of LS occurs when the component lateral load capacity starts to deteriorate, which can be caused by rupture of vertical or horizontal bars, crushing of boundary or web concrete, and slip of lap-splices (when present). For CP, excessive

deterioration of the load carrying capacity needs to be avoided, which means avoiding rupture of a significant number of bars, the complete crushing of boundary elements or web, or failure of lap splices.

Table 1 also proposes specific acceptance criteria based on material strains for each damage mechanism. Acceptance criteria are defined in terms of steel strain (ε_s), concrete strain (ε_c) and other strain-related parameters, and their exact definition can vary slightly depending on the modeling approach and material constitutive models employed. Flexural cracking is controlled by limiting the strain of vertical steel, while shear cracking is controlled by limiting the tensile concrete strains of diagonal elements in a truss model or by limiting the maximum principal (tensile) strains in a continuum FE model. Compressive damage of unconfined concrete (in the cover and web) is related to the exceedance of the compressive strain at the peak strength (ε_o) or ultimate point (ε_u), while compressive damage of confined concrete is related to its ultimate strain (ε_{cu}). In the case of strain limits in the decaying branch of the stress-strain curve (ε_u and ε_{cu}), their values are obtained by applying softening regularization as in the numerical model, for consistency. Bar rupture in the steel stress-strain laws used in this study is controlled using a parameter D that depends on the inelastic work under tensile stress, which triggers a sudden loss of tensile resistance once this parameter reaches a critical value D_{cr}. Hence, the acceptance criteria for steel is defined in terms of this strain-related parameter D. Additional details about the concrete and steel constitutive models are provided in subsequent sections. Damage related to lap-splice slip is controlled by the maximum tensile strain that the lap splice can develop prior to failure ($\varepsilon_{s,max}$), as described in Deng et al. (2022).

Table 1. Acceptance criteria based on material damage and strain-related parameters

Performance level	Exceedance criteria based on material damage	Acceptance criteria
Immediate Occupancy (IO)	Large residual flexural cracking	$\varepsilon_s \leq 1.0\%$
	Large diagonal (shear) cracks	Truss model: $\varepsilon_{c,diag} \leq w_{cr}/L_d$ FE model: $\varepsilon_{c,1} \leq w_{cr}/L_d$
	Concrete cover spalling	$\varepsilon_{c,vert} \geq -\varepsilon_0$
Life Safety (LS)	First fracture of vertical or horizonal bar	$D \leq D_{cr}$
	Onset of confined concrete crushing	$\varepsilon_{c,2} \geq -0.75\varepsilon_{cu}$
	Onset of diagonal web crushing	Truss model: $\varepsilon_{c,diag} \geq -\varepsilon_0$ FE model: $\varepsilon_{c,2} \geq -\varepsilon_0$
	Onset of slip in lap splice	$\varepsilon_s \leq 0.75\varepsilon_{s,max}$ for $\varepsilon_{s,max} < \varepsilon_y$ $\varepsilon_s \leq 0.5\varepsilon_{s,max}$ for $\varepsilon_{s,max} > 1.5\,\varepsilon_y$
Collapse Prevention (CP)	Fracture of more than 50% of boundary vertical bars in one boundary region or 50% of horizontal bars along a height equal to the wall length	$D \leq D_{cr}$ (in 50% of boundary/horizontal bars)
	Severe confined concrete crushing	$\varepsilon_{c,2} \geq -\varepsilon_{cu}$
	Severe diagonal web crushing	Truss model: $\varepsilon_{c,diag} \geq -\varepsilon_u$ FE model: $\varepsilon_{c,2} \geq -\varepsilon_u$
	Failure of lap splice (if present)	$\varepsilon_s \leq \varepsilon_{s,max}$

Note: $\varepsilon_{c,diag}$ concrete strain in diagonal element, $\varepsilon_{c,vert}$ vertical concrete strain, $\varepsilon_{c,1}$ maximum principal strain in concrete, $\varepsilon_{c,2}$ minimum principal strain in concrete, ε_y yield strain of steel, w_{cr} critical crack opening taken as 1.6 mm based on FEMA 306 (FEMA 1998), L_d length of diagonal element (truss model) or reference element length (FE model).

3. Simulation and performance evaluation using nonlinear truss models

3.1. Description of the method

The first method used to simulate and assess the response of planar RC walls is a version of the nonlinear truss model available in the program *FE-MultiPhysics* (Koutromanos 2023). The truss model represents a wall component using horizontal, vertical, and diagonal line elements, as shown in Figure 1a. Uniaxial stress-strain relations are used in each element to model the nonlinear response of concrete and steel reinforcement. Previous studies (Lu and Panagiotou 2014, Lu et al. 2016, Alvarez et al. 2020, Deng et al. 2021) have shown that this method and the beam-truss model, which is the 3D version of the truss model for non-planar walls, can accurately predict the response of walls exhibiting both flexural and shear failures. The implementation of

the truss model in *FE-MultiPhysics* features a four-node macro-element including two horizontal, two vertical, and two diagonal truss elements (see Figure 1a) to simplify pre- and post-processing.

The uniaxial constitutive law for unconfined and confined concrete was originally formulated by Lu and Panagiotou (2014) and is presented in Figure 1b. In the uniaxial compressive response, strength deterioration occurs when the strain magnitude surpasses ε_o and ε_{co} for unconfined and confined concrete, respectively. Beyond this point, concrete exhibits linear softening until reaching strain values equal to ε_u and ε_{cu} for unconfined and confined concrete, respectively. The effects of confining steel in the compressive stress-strain curve are calculated using the Mander model (Mander et al. 1988, Karthik and Mander 2011). The post-cracking tensile response is described by an exponential curve. In the case of diagonal truss elements, the concrete constitutive law also accounts for the effects of the transverse tensile strains on compressive resistance by means of a reduction coefficient, β, as depicted in Figure 1b. To avoid spurious mesh-size effects associated with localization, the softening branches of the compressive and tensile stress-strain relations are regularized using a reference length L_{ref} (Lu and Panagiotou 2014). The values of L_{ref} are defined based on the size of the test specimens used to calibrate the respective laws: L_{ref} is 600 mm for horizontal and vertical elements with unconfined concrete, 850 mm for inclined elements, and 450 mm for vertical elements with confined concrete (Deng et al. 2021).

Steel reinforcement is modeled using a uniaxial constitutive law proposed by Kim and Koutromanos (2016). This law was formulated to reproduce the cyclic response of steel reinforcement, including the effects of buckling and bar rupture. The hysteretic stress-strain response in absence of buckling and rupture is calculated with equations proposed by Dodd and Restrepo (1995), implemented by Kim and Koutromanos (2016) using a non-iterative stress-update algorithm. Bar buckling reduces the effective compressive stress of the bar using a criterion that depends on L_b/d_b (buckling length-to-bar diameter ratio) ratio, where this ratio is calculated based on the procedure proposed by Dhakal and Maekawa (2002). To model bar rupture, a parameter D related to the amount of inelastic work done in tension, defined in Kim and Koutromanos (2016), is employed. Once the parameter D reaches a critical value D_{cr}, the resistance drops to zero to simulate rupture (see Figure 1c). The value of D_{cr} can be calibrated to match the instant of bar rupture in a monotonic tensile test.

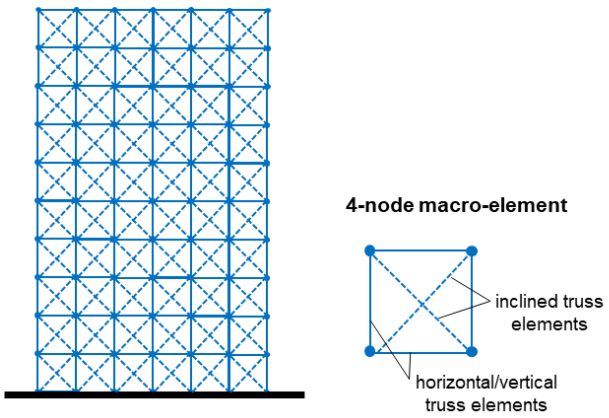

(a) Nonlinear truss scheme

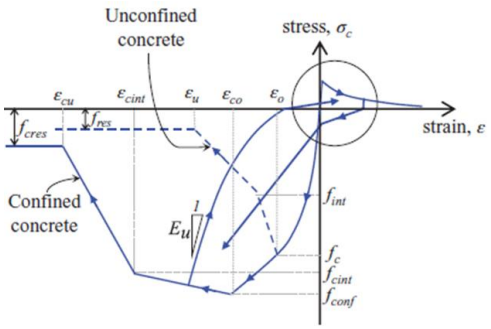

(b) Uniaxial law for concrete (Lu and Panagiotou 2014)

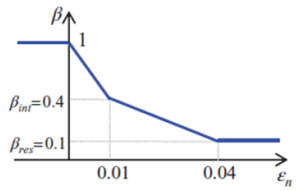

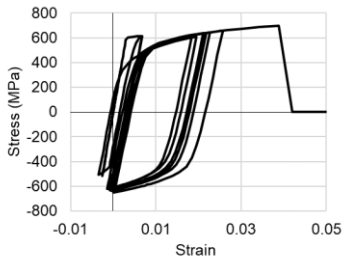

(c) Sample uniaxial response of steel

Figure 1. Nonlinear truss model and material laws

FE-Multiphysics includes a feature to correct a spurious effect of the method related to the compression resistance of wall boundaries. Specifically, the overlap of inclined and vertical elements in a 4-node macro-element can lead to an overestimation of the compressive resistance of a boundary region. To address this issue, the stresses in vertical and inclined elements in this region are scaled so that the resultant stress matches the uniaxial compressive law. In addition, concrete resistance is completely eliminated once the equivalent minimum principal strain of the macro-element reaches the ultimate compressive strain of the concrete.

3.2. Simulation of test specimens

Numerical analyses of four large-scale tests on planar RC walls are presented to illustrate the capability of the truss modeling scheme to simulate different types of failures. They include three wall specimens with rectangular sections tested by Dazio et al. (2009) and Tran and Wallace (2015), and one wall with barbell section tested by Oesterle et al. (1979). The two walls tested by Dazio et al. (2009) exhibited a flexure-dominated behavior, one failed due to vertical bar rupture (specimen WSH3) and the other due to crushing of the boundary element (specimen WSH6). Specimen RW-A20-P10-S38 tested by Tran and Wallace (2015) initially presented a flexure-dominated response, but eventually failed in diagonal tension. The barbell wall (specimen B6) tested by Oesterle et al. (1979) failed due to diagonal crushing of the web. These four walls were previously modeled by Deng et al. (2021) using a version of the truss model that did not include the stress correction due to overlap of vertical and inclined line elements described in the previous section. The rest of modeling parameters and material properties used here are described in Deng et al. (2021).

The force-displacement curves obtained from the analysis of the four walls are presented and compared with experimental results in Figure 2. As shown, the truss model is in good agreement with the experimental force-displacement responses. The model is also capable of estimating the dominant type of failure and deformation demand at failure: bar rupture after reaching a maximum drift ratio of 2% for WSH3, crushing of a boundary element at a drift ratio close to 2% for WSH6 (1.9% in the test, 2.2% in the model after experiencing a bar rupture in the same cycle), diagonal tension failure with rupture of multiple horizontal bar at a drift ratio near 3% for RW-A20-P10-S38, and diagonal web crushing at a drift ratio of around 1.5% for B6.

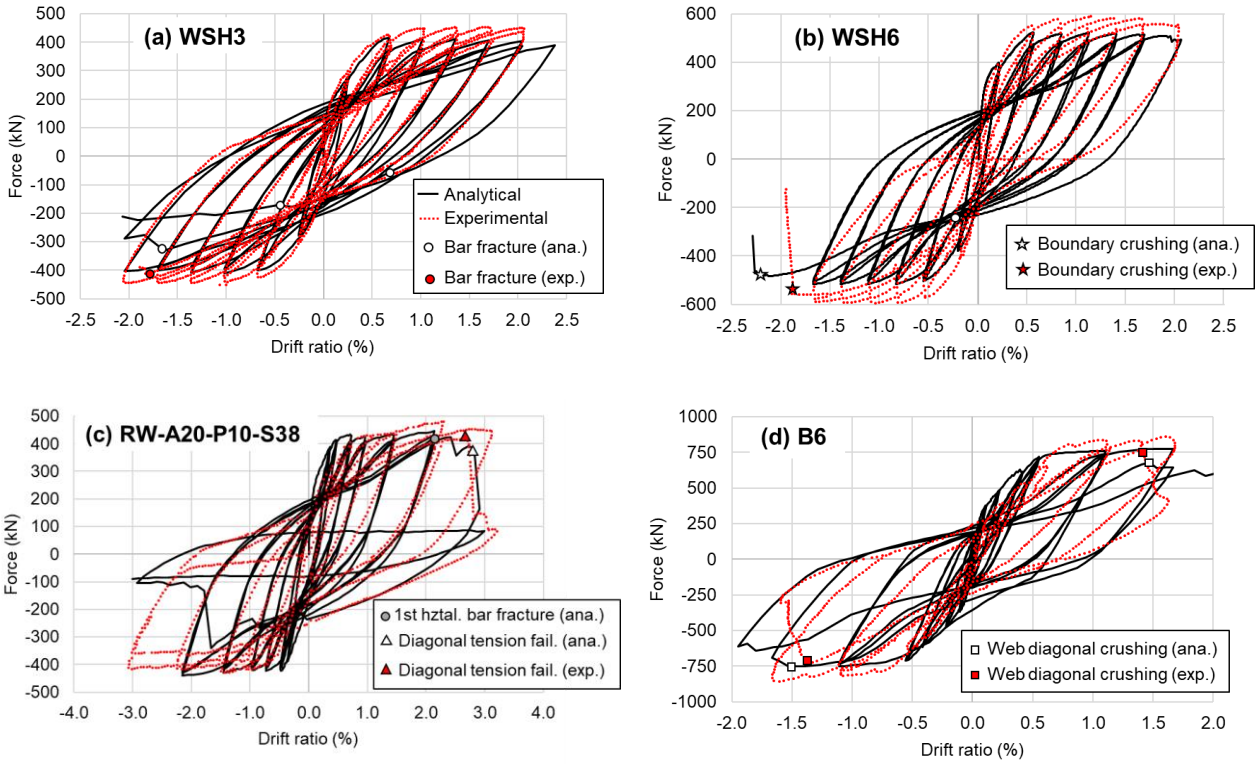

Figure 2. Force-displacement responses obtained with nonlinear truss models

The maximum principal strains and deformed shapes of the wall models at failure are plotted in Figure 3 to illustrate the type of damage and cracking pattern obtained by the models. The map of maximum principal

strains of WSH3 and WSH6 is typical of walls behaving in flexure, which exhibit horizontal and diagonal cracking. The large concentration of tensile strains along a diagonal band in RW-A20-P10-S38 corresponds to a diagonal tension failure like that observed in the test. The vertical band at the interface between the web and pilaster in the barbell wall B6 coincides with the formation of a major crack at this interface and the web crushing observed in the test.

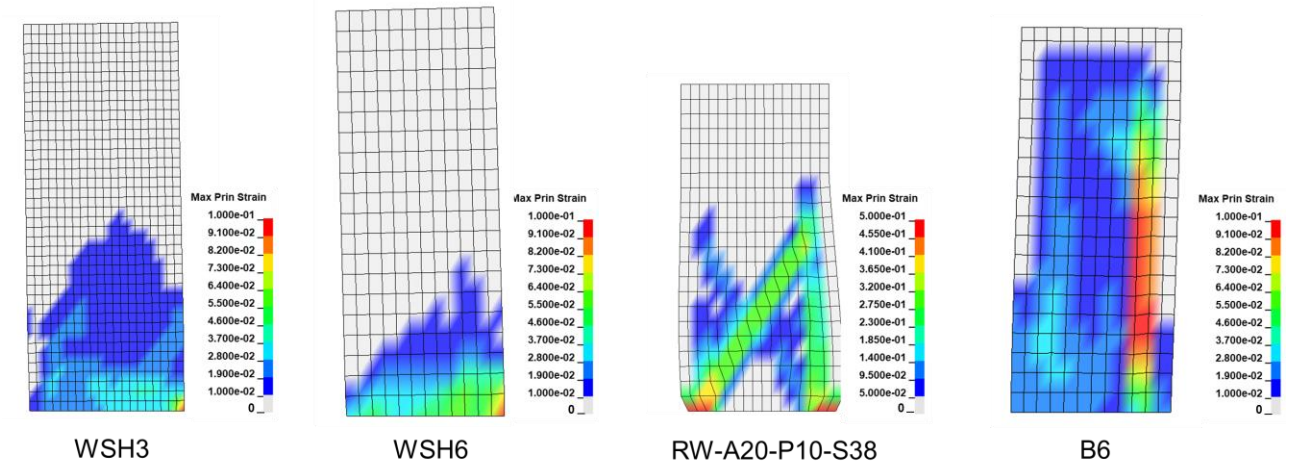

Figure 3. Maximum principal strains at failure

3.3. Performance evaluation

The strain-based performance limits have been evaluated for the four wall analyses presented in the previous section. To this end, the material strains and strain-related parameters obtained from the numerical analyses were compared to the performance thresholds defined in Table 1 to determine the point at which each wall specimen exceeds the LS, IO and CP levels. Figure 4 presents the resulting performance limits in the force-displacement diagrams. This figure also compares the numerical results with the backbone curves and performance limits obtained with the ASCE/SEI 41-17 (ASCE 2017), as well as the performance limits obtained using Eurocode 8-3 (CEN 2005) for damage limitation (DL), significant damage (SD), near collapse (NC). The definitions of DL, SD, and NC are essentially equivalent to IO, LS, CP, respectively. The drift ratios at which these three damage states are exceeded are calculated based on chord rotation equations from Eurocode 8-3 (CEN 2005) for flexure-dominated walls with additional assumptions described in Plaza (2022) to account for mixed flexure-shear behavior.

The simulation-based method indicates that all four walls exceed IO due to cover spalling. As shown in Figure 4, the IO limit points in the force-displacement curves are very close to the effective yield point of the curves, which marks the significant loss of stiffness that needs to be avoided at this performance level. The LS level is exceeded due to a variety of damage modes: first vertical bar rupture (WSH3 and WSH6), first rupture of horizontal bar (RW-A20-P10-S38) and onset of web crushing (B6). The LS limit points are located at the start of the decay of the lateral load capacity, consistent with what is typically assumed in ASCE/SEI 41-17 (ASCE 2017). Finally, CP is exceeded due to multiple ruptures of vertical bars for WSH3 and horizontal bars for RW-A20-P10-S38, severe confined concrete crushing in the case of WSH6, and severe web crushing in specimen B6. The CP limit points are consistent with the decay of lateral load capacity observed in the force-displacement curves.

Figure 4 shows that the simulation-based method and ASCE/SEI 41-17 (ASCE 2017) provide very similar force-displacement envelopes and performance limits for the walls failing in flexure, WSH3 and WSH6. For the walls failing in shear (RW-A20-P10-S38 and B6), ASCE/SEI 41 (ASCE 2017) estimates a significantly lower deformation capacity than the numerical results, which are more consistent with experimental results. Eurocode 8-3 (CEN 2005) results in deformation limits that are very similar to ASCE/SEI 41-17 (ASCE 2017) in all fours walls.

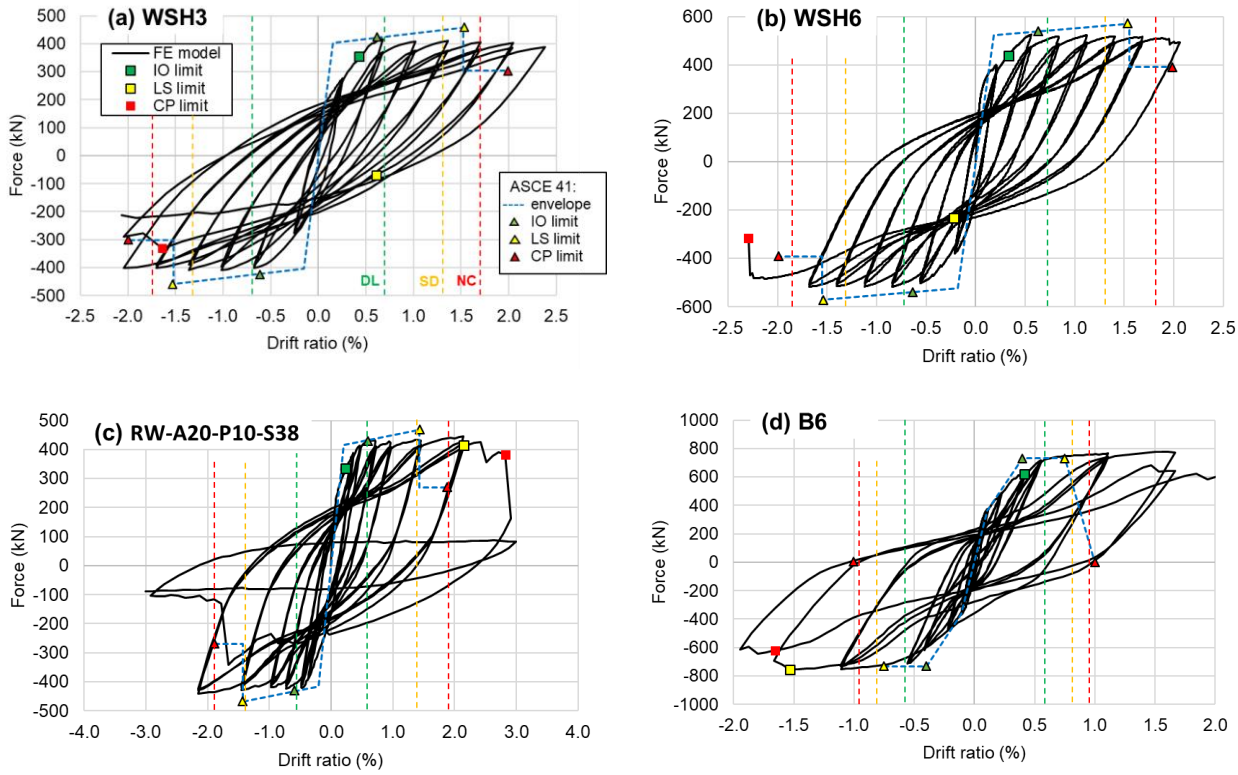

Figure 4. Performance limits in RC wall specimens according to nonlinear truss models

4. Simulation and performance evaluation using continuum FE models

4.1. Description of the method

Two-dimensional (2D) continuum FE models of planar RC walls have also been used to simulate and assess the response of planar walls. The models have been developed in the software DIANA 10.7 (DIANA 2023). Plane stress, four-node linear quadrilateral element are used to model concrete. Reinforcement is modeled with line elements embedded in concrete (perfect bond is assumed). Figure 5 presents the modeling scheme of a wall component.

The constitutive law for concrete is the total strain crack model available in DIANA, developed along the lines of Modified Compression Field Theory (Vecchio and Collins 1986). For compression, inelastic behavior is represented by a parabolic constitutive law whose shape is defined in terms of compressive fracture energy, as shown in Figure 5b. The material model parameters have been consistently calibrated based on the reported compressive strength of concrete, following the guidelines by Hendriks and Roosen (2020) and additional assumptions described next. The effect of transverse cracking in compression response is governed by a reduction factor β defined by the equation proposed by Vecchio and Collins (1986). Given the 2D nature of the model, the effect of confinement in the compressive response cannot be naturally captured in the model. For this reason, the shape of the uniaxial compressive stress-strain law for confined concrete is defined based on Mander´s model, from which the input compressive fracture energy is calculated. The tensile behavior of concrete is modeled with a rotating smeared crack approach. An exponential tensile curve is used requiring definition of the fracture energy, as shown in Figure 5b. Recommendations from the Hendriks and Roosen (2020) and the fib model Code 2010 (fib 2013) have been used to calibrate the tensile curve. Both the compression and tension softening response are regularized based on the element's equivalent length. The equivalent length or crack bandwidth is determined using the projection method proposed by Govindjee et al. (1995).

The stress-strain response of steel reinforcement is modeled using a Menegotto-Pinto model (Menegotto and Pinto 1973, Filippou et al. 1983) modified to account for bar rupture, as shown in Figure 5c. The bar rupture criterion is similar to that of Kim and Koutromanos (2016), and comprises a parameter *D* that depends on the inelastic tensile work and maximum strain amplitude to determine the point at which the bar loses resistance

when D reaches a critical value D_{cr}. This failure criterion was calibrated and verified in Fawaz and Murcia-Delso (2021). The steel model has been implemented in DIANA through a user subroutine.

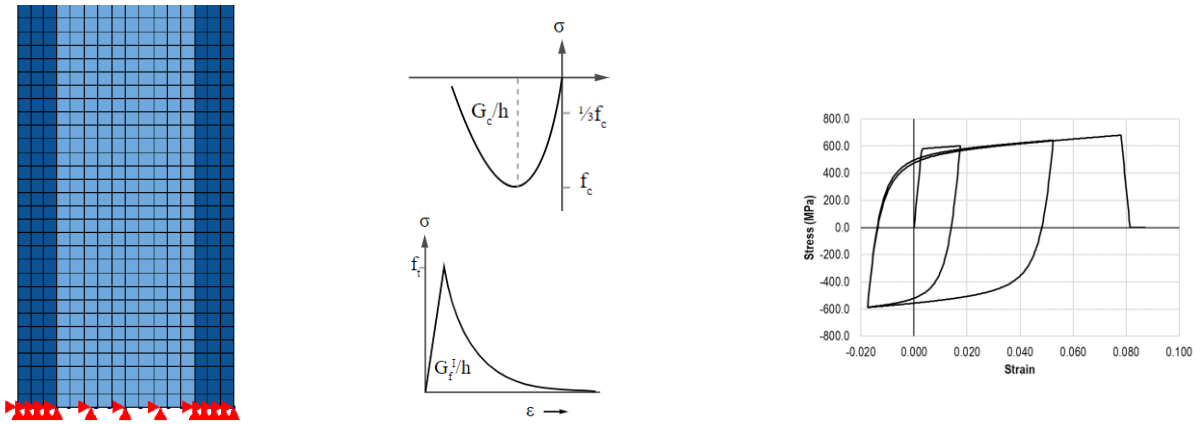

(a) 2D FE model *(b) Compressive and tensile curves (DIANA 2023)* *(c) Sample uniaxial response of steel*

Figure 5. 2D FE models and material laws

Additional details about the 2D FE modeling strategy and the calibration of the constitutive models presented here are provided in Luna (2022).

4.2. Simulation of test specimens

The four wall tests previously described have been modeled using the proposed 2D continuum FE scheme. Figure 6 compares the analytical and experimental force-displacement curves. As shown, overall good accuracy is also achieved regarding the force-displacement responses and maximum drifts at failure. The boundary crushing failure of WSH6 and web crushing failure of B6 are well represented, along with their fast load drops. In contrast, the failure modes of WSH3 and RW-A20-P10-S38 are not accurately represented in the FE model. For WSH3, the model exhibits boundary crushing prior to the first rupture of a vertical bar. In For RW-A20-P10-S38, the failure is dominated by the diagonal crushing of the web instead of diagonal tension even though there are some fractures of horizontal bars.

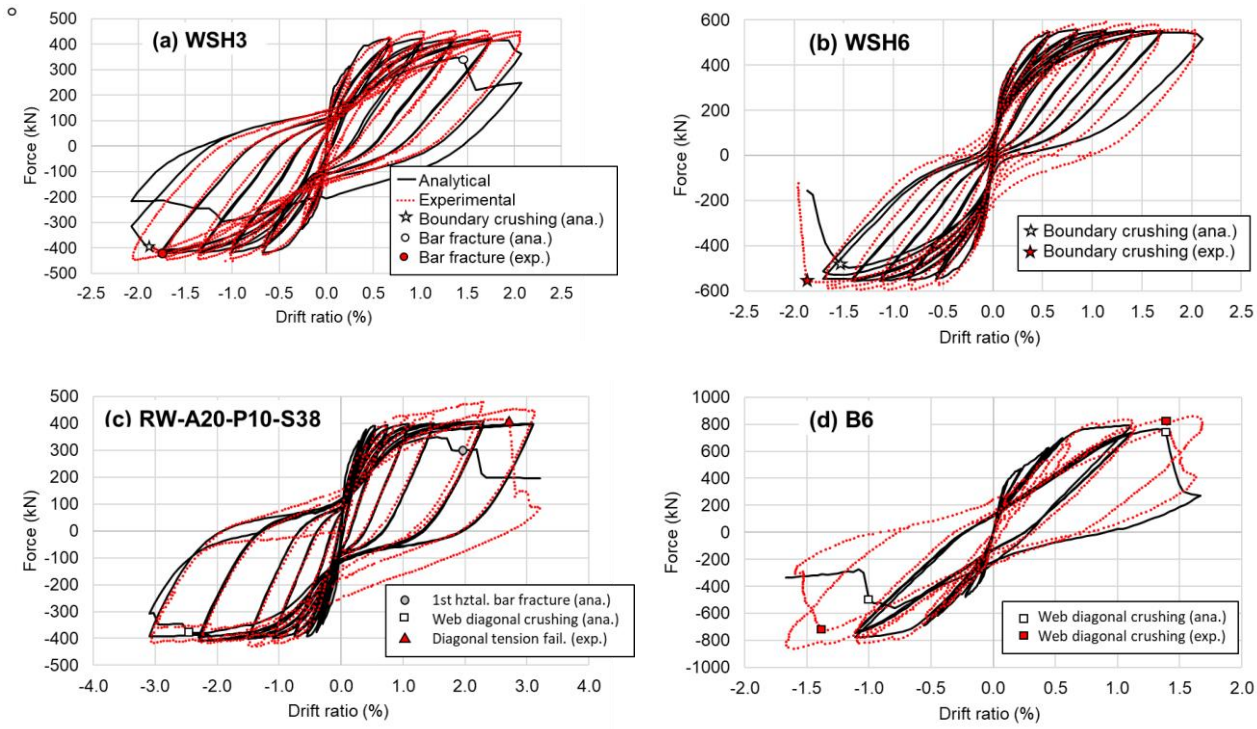

Figure 6. Force-displacement responses obtained with FE models

Figure 7 presents the distribution of crack widths in the concrete and deformed shapes at failure. The map of crack widths for WSH3 and WSH6 are in good agreement with the flexure-dominated behavior of these two walls, and the wide vertical crack band of B6 is consistent with that obtained in the test at the boundary between pilaster and web. For RW-A20-P10-S38, the crack pattern and deformed shape indicate the web crushing along a vertical band, instead of the diagonal crack obtained in the test.

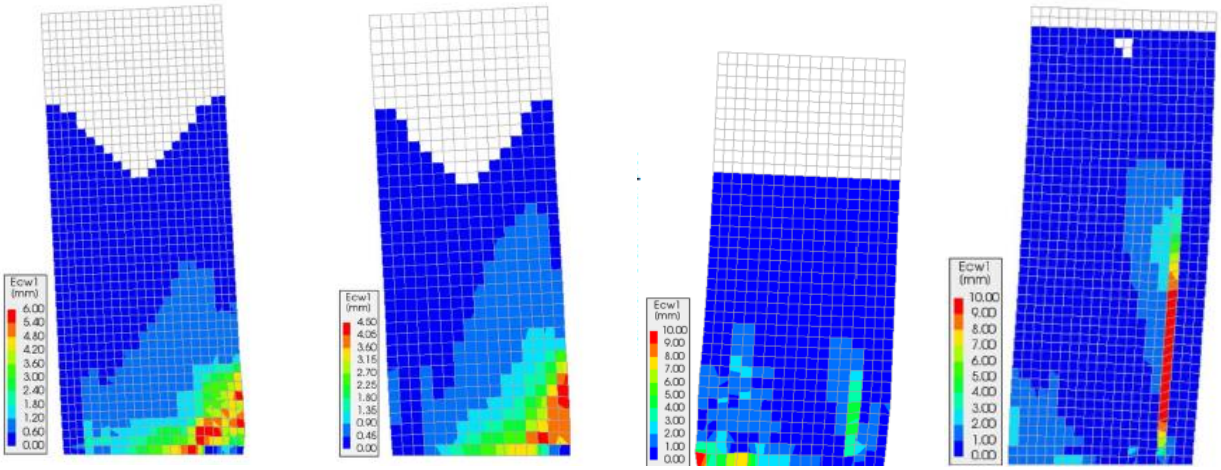

Figure 7. Crack widths obtained from FE models at failure

4.3. Performance evaluation

The strain-based performance limits have been evaluated using the results of the FE models presented in the previous section, following the same procedure as for the truss models based on the criteria of Table 1. Figure 8 presents the resulting performance limits in the force-displacement diagrams along with backbone curves from ASCE/SEI 41-17 (ASCE 2017). The performance limits obtained from ASCE/SEI 41-17 (ASCE 2017) for IO, LS, CP, and from Eurocode 8-3 (CEN 2005) for DL, SD and NC are also presented in Figure 8.

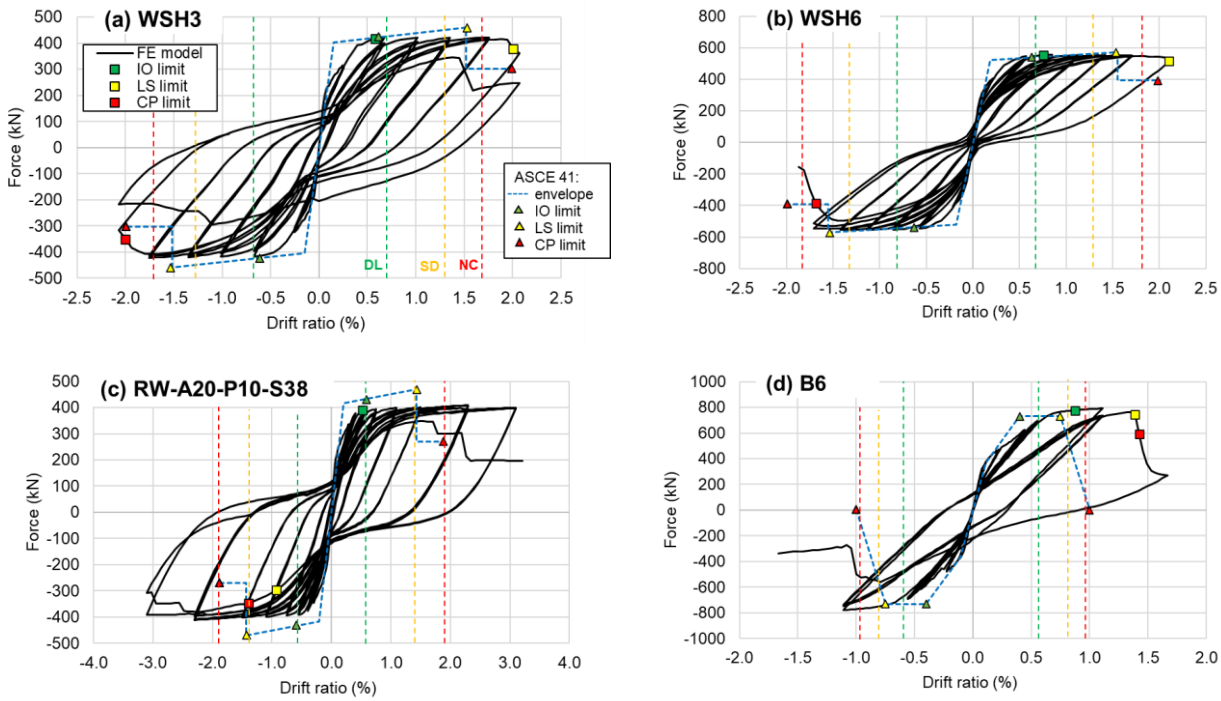

Figure 8. Performance limits in RC wall specimens according to 2D FE models

The FE models indicate that IO is exceed due to cover spalling or wide flexural cracking. As shown in Figure 4, IO is exceeded shortly after the force-displacement curve reaches its effective yield point, consistent with the definition of this limit state. The LS level is exceeded due to onset confined concrete crushing for WSH3 and WSH6, and due to onset of web crushing for RW-A20-P10-S38 and B6. These are consistent with the dominant failure modes obtained in these models and also coincides with the start of the decay of the lateral load capacity. In all four cases, there is a rapid damage evolution and load decay leading to exceeding CP at a drift level very close to LS. This is explained by the brittleness of the concrete crushing mechanism governing the failures in these models.

Like for the truss models, the deformation limits obtained for FE models for each of the performance levels are in line with those obtained with ASCE/SEI 41-17 (ASCE 2017) and Eurocode 8-3 (CEN 2005) for the two walls failing in flexure, while significant differences are observed for the two walls failing in shear due to the underestimation of deformation capacity obtained by the standards in these specific cases.

5. Conclusions

A new framework has been presented for the seismic evaluation of RC structural walls which is based on advanced numerical simulation techniques and the use of strain-based acceptance criteria. The proposed approach relies on the ability of the numerical models in reproducing the main inelastic mechanisms in RC walls, including different types of failures. A set of limits based on material strains or strain-related parameters for concrete and steel have been established for Immediate Occupancy (IO), Life Safety (LS) and Collapse Prevention (CP) levels. The use of this framework has been demonstrated for two different types of numerical models: nonlinear truss models and 2D continuum finite element (FE) models. Four test specimens exhibiting flexure- or shear-dominated failures from tests reported in the literature have been modeled with these two methods. The results obtained are in good agreement with the cyclic lateral response of the wall specimens, including the deformation at which the failures occurred and the general types of failure (flexure vs. shear). Both the truss models and FE models are capable of reproducing vertical bar ruptures, boundary crushing and web crushing failures, but only the truss model replicates the diagonal tension failure observed in one of the tests. In addition, truss models were faster to run than the FE models (between 2 and 3 times faster for models with similar mesh size). Based on the four walls analyzed it is also concluded that the proposed strain-related limits are consistent with the decay of stiffness and/or strength expected at the component level at the three performance levels. For shear failures, these limits are more consistent with experimental observations than those obtained with ASCE/SEI 41 (ASCE 2017) and Eurocode 8-3 (CEN 2005).

The proposed framework has promise as a higher-tier alternative to current standard approaches for the seismic assessment of wall buildings. In this regard, the truss model is found to be preferable for evaluating entire structural systems, as it combines high accuracy at lower computational cost than continuum FE models. Beam-truss models have already been used for nonlinear static and dynamic analyses of entire RC wall buildings (Zhang et al. 2017, Mavros et al. 2022, Mavros et al. 2023). The new evaluation framework can also be used as a complement to the nonlinear ASCE/SEI 41 approach, as it can be employed to simulate wall components in order to calibrate simpler models (backbone curves) and acceptance criteria based on drift ratio or hinge ratio. Hence, it could contribute to replace or reduce the need for physical testing for determining alternative modeling and acceptance limits. Still, further verification and refinement of the strain-based performance limits is needed to increase the reliability of the proposed method.

6. Acknowledgements

The research presented in this paper was supported by the National Institute of Standards and Technology (NIST) under award No. 70NANB19H060 and by the Spanish Research Agency (MCIN/AEI /10.13039/501100011033) and European Union NextGenerationEU/PRTR under project STREIN (CNS2022-135574). Any opinions and findings presented in this paper are those of the authors alone, and do not necessarily reflect the opinions of the sponsors.

7. References

Alvarez R., Restrepo J.I., Panagiotou M. (2020). RC wall plastic hinge out-of-plane buckling: analysis using the nonlinear beam-truss model, *ASCE Journal of Structural Engineering*, 146(12):04020274.1–20.

ASCE (2017). *Seismic Rehabilitation of Existing Buildings*, ASCE/SEI 41-17, American Society of Civil Engineers, Reston, VA, United States.

CEN (2005). *EN 1998-3:2005. Eurocode 8: Design of structures for earthquake resistance - Part 3: Assessment and retrofitting of buildings*, Comité Européen de Normalisation, Brussels.

Dazio A., Beyer K., Bachmann H. (2009). Quasi-static cyclic tests and plastic hinge analysis of RC structural walls, *Engineering Structures*, 31(7): 1556-1571.

Deng X., Koutromanos I., Murcia-Delso J., Panagiotou M. (2021). Nonlinear truss models for strain-based seismic evaluation of planar RC walls, *Earthquake Engineering and Structural Dynamics*, 50: 2939–2960.

Deng X., Murcia-Delso J., Koutromanos I., Panagiotou M. (2022). Nonlinear truss modeling and strain-based evaluation of RC walls considering lap-splice failure effects, *3rd European Conference on Earthquake Engineering and Seismology*, Bucharest, Romania.

DIANA FEA BV (2022). DIANA Documentation Release 10.5, Thijsseweg 11, 2629 JA Delft, The Netherlands.

Dhakal R.P., Maekawa K. (2002). Path-dependent cyclic stress-strain relationship of reinforcing bars including buckling, *Engineering Structures*, 24(11):1383-1396.

Dodd L.L., Restrepo-Posada J.I. (1995). Model for predicting cyclic behavior of reinforcing steel, *ASCE Journal of Structural Engineering*, 121(3):433-445.

Fawaz G., Murcia-Delso J. (2021). Three-dimensional finite element modeling of RC columns subjected to cyclic lateral loading, *Engineering Structures*, 239:112291.

FEMA (1998). *Evaluation of earthquake-damaged concrete and masonry wall buildings: basic procedures manual, FEMA 306*. Prepared by the Applied Technology Council for the Federal Emergency Management Agency, Washington, DC, United States.

fib, Federation Internationale du Beton (2010). *Model Code 2010 Volume* 1, Lausanne, Switzerland.

Filippou F.C., Popov E.P., Bertero V.V. (1983). *Effects of bond deterioration on hysteretic behavior of reinforced concrete joint* (EERC 83-19). Earthquake Engineering Research Center, University of California, Berkeley.

Govindjee S., Kay G. J., Simo J.C. (1995). Anisotropic Modelling and Numerical Simulation of Brittle Damage in Concrete, *International Journal for Numerical Methods in Engineering*, 38: 3611-3633.

Karthik M.M., Mander J.B. (2011). Stress-block parameters for unconfined and confined concrete based on a unified stress-strain model, *Journal of Structural Engineering*, 137(2):270-273.

Kim S., Koutromanos I. (2016). Constitutive model for reinforcing steel under cyclic loading, *Journal of Structural Engineering*, 142(12):1-14.

Koutromanos I. (2023). FE-*MultiPhys: A Finite Element Program for Nonlinear Analysis of Continua and Structures. Version 2023.* Virginia Polytechnic Institute and State Univ., Blacksburg, VA, United States.

Hendriks M.A., Roosen M. (2020). *Guidelines for nonlinear finite element analysis of concrete structures*, Rijkswaterstaat Tech. Doc. (RTD), Rijkswaterstaat Cent. Infrastructure, RTD, 1016-12020.

Mander J.B., Priestley M.J.N., Park R. (1988). Theoretical stress-strain model for confined concrete, *ASCE Journal of Structural Engineering*, 114(8): 1804-1826

Menegotto M., Pinto P.E. (1973). Method of Analysis for Cyclically Loaded Reinforced Concrete Plane Frames Including Changes in Geometry and Non-Elastic Behavior. *Proceedings of IABSE Symposium on Resistance and Ultimate Deformation of Structures Acted upon by Well-Defined Loads*.

Mavros M., Panagiotou M., Koutromanos I., Alvarez R., Restrepo J.I. (2022). Seismic analysis of a modern 14-story reinforced concrete core wall building system using the BTM-shell methodology, *Earthquake Engineering and Structural Dynamics*, 51(6): 1540-1562.

Mavros M., Panagiotou M., Koutromanos I., Restrepo J.I. (2023). Nonlinear dynamic seismic analysis of a modern concrete core wall building in Los Angeles using the BTM-shell methodology, E*arthquake Engineering and Structural Dynamics*, 52(14), 4415-4441.

Lu Y., Panagiotou M. (2014). Three-dimensional cyclic beam-truss model for nonplanar reinforced concrete walls, *ASCE Journal of Structural Engineering*, 04013071:1-11.

Lu Y., Panagiotou M., Koutromanos I. (2016). Three-dimensional beam-truss model for reinforced concrete walls and slabs—part 1: modeling approach, validation, and parametric study for individual reinforced concrete walls, *Earthquake Engineering and Structural Dynamics*, 45(9):1495-1513.

Luna, P. (2022). *Numerical Modeling of the Cyclic Response of Reinforced Concrete Walls using Continuum Finite Element Models*, MS Thesis. Universitat Politècnica de Catalunya, Barcelona, Spain.

Oesterle R., Aristizabal-Ochoa J., Fiorato A., Russel H., Corley W. (1979). *Earthquake Resistant Structural Walls - Tests of Isolated Walls Phase II,* Report to the National Science Foundation. Construction Technology Laboratories, Portland Cement Association, Skokie, IL, United States.

Panagiotou M., Restrepo J. (2011). Displacement-based method of analysis for regular reinforced-concrete wall buildings: application to a full-scale 7-story building slice tested at UC–San Diego, *ASCE Journal of Structural Engineering*, 137(6):677-690.

Plaza, R. (2022). *Comparative analysis of seismic evaluation methods for RC walls in ASCE 41-17 and Eurocode 8-3*, MS Thesis. Universitat Politècnica de Catalunya, Barcelona, Spain.

Priestley M.J.N., Calvi G.M., Kowalsky M.J. (2007). *Displacement-Based Seismic Design of Structures*. Pavia, Italy: IUSS Press.

Tran T.A., Wallace J.W. (2015). Cyclic testing of moderate-aspect-ratio reinforced concrete structural walls, *ACI Structural Journal*, 112(6):653-666.

Vecchio F.J., Collins M.P. (1986). Modified Compression-Field Theory for Reinforced Concrete Elements Subjected To Shear, *Journal of the American Concrete Institute*, 83(2): 219-231.

Zhang P., Restrepo J.I., Conte J.P., Ou J. (2017). Nonlinear finite element modeling and response analysis of the collapsed Alto Rio building in the 2010 Chile Maule earthquake, Structural Design of Tall and Special Buildings, 26(16): e1364.